# Switching and Sensing Spin States of Co–Porphyrin in Bimolecular Reactions on Au(111) Using Scanning Tunneling Microscopy

**Howon Kim,[†,§] Yun Hee Chang,[‡,§] Soon-Hyeong Lee,[†] Yong-Hyun Kim,[‡,*] and Se-Jong Kahng[†,*]**

[†]Department of Physics, Korea University, 136-713, Seoul, Republic of Korea and [‡]Graduate School of Nanoscience and Technology, KAIST, 305-701, Daejeon, Republic of Korea. [§]These authors contributed equally to this work.

**ABSTRACT** Controlling and sensing spin states of magnetic molecules at the single-molecule level is essential for spintronic molecular device applications. Here, we demonstrate that spin states of Co–porphyrin on Au(111) can be reversibly switched over by binding and unbinding of the NO molecule and can be sensed using scanning tunneling microscopy and spectroscopy (STM and STS). Before NO exposure, Co–porphyrin showed a clear zero-bias peak, a signature of Kondo effect in STS, whereas after NO exposures, it formed a molecular complex, NO–Co–porphyrin, that did not show any zero-bias feature, implying that the Kondo effect was switched off by binding of NO. The Kondo effect could be switched back on by unbinding of NO through single-molecule manipulation or thermal desorption. Our density functional theory calculation results explain the observations with pairing of unpaired spins in $d_{z^2}$ and pp$\pi$* orbitals of Co–porphyrin and NO, respectively. Our study opens up ways to control molecular spin state and Kondo effect by means of enormous variety of bimolecular binding and unbinding reactions on metallic surfaces.

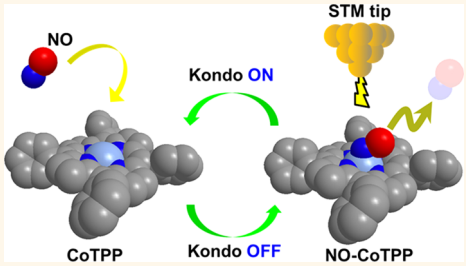


**KEYWORDS:** scanning tunneling microscopy · scanning tunneling spectroscopy · metalloporphyrin · nitric oxide · density functional theory · Kondo resonance

Controlling spin states of magnetic molecules is essential for spintronic molecular device applications.[1,2] An easy way to implement spin-state control in magnetic molecules is to provide another molecule to form a new chemical bond. When metalloporphyrins and phthalocyanines exothermically form axial or tilted binding structures with small gaseous molecules, NO, CO, and $O_2$, their magnetic moments systematically vary.[3−9] Orbital and spin structures of such systems have been extensively studied for the last four decades because their binding and unbinding reactions occur in dynamic processes of biological functions such as respiration, photosynthesis, and neurotransmission.[10−15] In the binding reactions, a metal at the center of metalloporphyrins and phthalocyanines transforms its coordination numbers from four to five or six, thereby inducing changes in the number of unpaired electrons and magnetic moments.[16−20] Recent X-ray magnetic circular dichroism (XMCD) experiments have demonstrated on a ferromagnetic Ni(100) substrate that the magnetic ordering of unpaired electrons of Co in Co–porphyrin, induced by the ferromagnetic substrate, disappears after NO binding.[5] On Ag(111), ultraviolet photoelectron and scanning tunneling spectroscopy (STS) experiments showed that both electronic and spin states of Co–porphyrins changed with NO coordination.[4,6,21,22] Our group has recently reported that Co–porphyrin on Au(111) showed Kondo effect using scanning tunneling microscopy (STM) and STS,[23] which originates from the exchange coupling between unpaired spins of magnetic molecules and conduction electrons of metal substrates.[24−33] However, there has been no attempt to control the Kondo effect in this system by using binding and unbinding reactions of small molecules.[34,35]

In this paper, we demonstrate that the Kondo effect of tetrakisphenylporphyrin–Co (CoTPP) on Au(111) can be reversibly switched off and on by binding and unbinding of the NO molecule, respectively, using

* Address correspondence to sjkahng@korea.ac.kr, yong.hyun.kim@kaist.ac.kr.

Received for review July 30, 2013 and accepted September 4, 2013.

**Published online September 04, 2013**
**10.1021/nn4039595**

STM and STS. Upon NO exposure, three-lobed CoTPP transforms to ring-shaped NO−CoTPP in STM images. The former showed a clear zero-bias peak, a signature of Kondo effect, in STS, but the latter did not, implying that the Kondo effect was switched off by NO binding. We also showed that a single NO molecule could be detached from CoTPP by using STM manipulations or thermal desorption, thereby the Kondo effect could be switched on. The observed results were explained with our density functional calculation results. Our experiments showed that the Kondo effect in an entire sample could be simultaneously and remotely switched off by using gaseous NO, which corresponded to the resetting procedures of spintronic memory and sensor devices.

## RESULTS AND DISCUSSION

Molecular islands of randomly mixed CoTPP and $H_2$TPP (50:50) were prepared at 150 K and imaged at 80 K on Au(111), as shown in Figure 1a. We used $H_2$TPP to confirm that the center metal of porphyrin was essential for NO binding in CoTPP. STM images obtained at −0.8 eV show a three-lobed structure for CoTPP and a depressed center structure for $H_2$TPP. Two-fold symmetry of CoTPP can be explained by saddle-type deformations on metal substrates.[23,36] In STS curves of Figure 1b obtained at two locations within the molecules, $H_2$TPP has a peak at −1.0 eV, the highest occupied molecular orbital (HOMO), and at +1.5 eV, the lowest unoccupied molecular orbital (LUMO). In STS curves of Figure 1c, CoTPP also has two peaks at the same energies, implying that these states originate from the macrocycle of porphyrin. CoTPP had two additional peaks observed near the Fermi level due to the presence of the Co atom. The peak at −0.2 eV is strong at the locations of the two pyrrolic rings. The peak at the Fermi level is assigned to the Kondo resonance state, in agreement with previous STS studies of Co−porphyrin molecules.[23−27] The asymmetric shape of the Kondo peak was fitted with a Lorentzian-like curve, which is based on the Fano formula, to yield the Kondo temperature of 225 K.[37,38] This Kondo temperature lies within the reasonable range compared with those of other reports on molecular Kondo effect.[23−31,33]

When the molecular islands were exposed to NO gas with the STM tip retracted, the three-lobed structures of some CoTPPs were replaced by bright ring structures. Figure 2 shows consecutive STM images obtained from the same area before and after the NO exposures. Bright ring structures were explained by the tilted binding of a NO that precesses around in NO−CoTPP nitrosyl complexes.[39] To confirm if the proposed control of Kondo effect was successfully implemented by the bimolecular binding reactions, we performed local manipulations using a voltage-sweep method. The STM tip was located close to the center

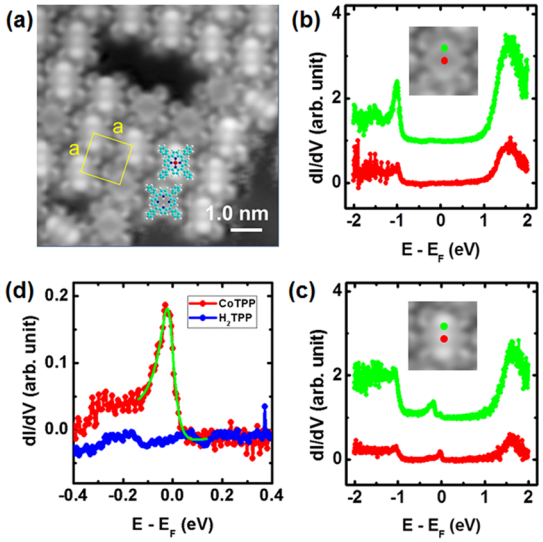


**Figure 1. (a) Typical STM image of two-dimensional molecular islands of mixed CoTPP and $H_2$TPP, with tunneling current, $I_T$ = 0.1 nA, and the sample bias, $V_s$ = −0.8 eV. A molecular unit cell is depicted as a yellow square with the lattice constant a = 1.40 ± 0.01 nm. The atomic models of $H_2$TPP and CoTPP are overlaid. The red, blue, cyan, and white spheres indicate cobalt, nitrogen, carbon, and hydrogen atoms, respectively. Tunneling spectra for (b) $H_2$TPP and (c) CoTPP at two different positions indicated in the inset STM images of an individual $H_2$TPP and CoTPP. The initial tunneling conditions are $I_T$ = 0.35 nA and $V_s$ = 0.65 eV. (d) Enlarged tunneling spectra at the centers of molecules for (b) $H_2$TPP (in blue) and (c) CoTPP (in red). The green line in (d) shows a Lorentzian fitting with asymmetry parameter, $|q|$ = 3.06, resonance energy, $E_K$ = −10.9 meV, and Kondo temperature, $T_K$ = 225 K.**

of the molecule, and then the sample voltage was increased while holding the feedback loop open so that the tip maintained a constant distance from the molecule. An abrupt jump in tunneling current was observed at about +0.7 eV, as shown in Figure 3a. Figure 3b,c shows two STM images that include the manipulated CoTPP molecule, obtained before and after the voltage sweep. The shape of the manipulated CoTPP molecule was recovered from the bright ring structure to the original three-lobed structure. After the change, the voltage was swept back to negative polarity but did not induce any more jumps. During the process of a voltage sweep, a differential conductance (d*I*/d*V*) spectrum was simultaneously obtained as shown in Figure 3d. The d*I*/d*V* spectrum showed a featureless curve near the Fermi level when the voltage was increased during the manipulation. This means that both Kondo effect and the state at −0.2 eV were switched off by the NO exposure. However, when the voltage was decreased again, the d*I*/d*V* spectrum showed the two distinctive peaks at the Fermi level and at −0.2 eV, confirming that the original structure of CoTPP and corresponding Kondo effect were recovered by the local manipulation. The amplitudes of these peaks are weaker than those in Figure 1 because of different tip−sample distances.

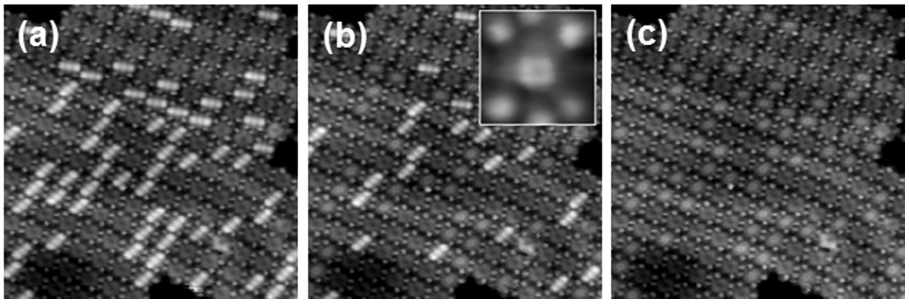


**Figure 2. Sequential STM images of a mixed molecular island of CoTPP and $H_2$TPP on Au(111) (a) before, (b) after 300 L, and (c) after 900 L exposure to NO at 80 K. The inset of (b) shows an enlarged STM image of a single NO−CoTPP. Comparing (a) with (b) and (c) shows that no $H_2$TPP is affected by NO exposures.**

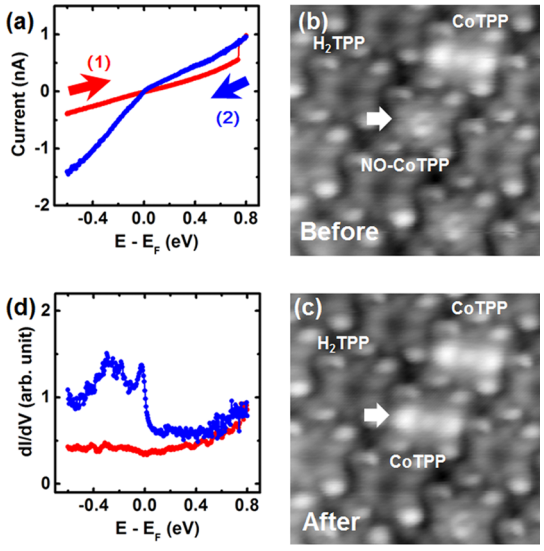


**Figure 3. (a) Current−voltage (*I*−*V*) curves obtained during STM manipulation procedure for a NO−CoTPP. At the center of a NO−CoTPP, the sample bias was swept from −0.4 to 0.8 eV (in red) while holding the feedback loop open, resulting in an abrupt increase in current at 0.7 eV. Afterward, the sample bias was swept back to negative polarity (in blue) with no abrupt change in current. The STM images obtained (b) before and (c) after the STM manipulation of (a). (d) d*I*/d*V* spectra recorded at the same time as the two *I*−*V* curves shown in (a).**

The local manipulation could be repeated without significantly influencing neighboring molecules, as demonstrated in sequential STM images obtained between each step of the manipulation in Figure 4. By the manipulation between Figure 4c,d, two CoTPP molecules exchange their shapes, implying that a NO molecule detached from the first CoTPP and reattached to the neighboring CoTPP. Very rarely, reattachment of NO released back from the tip was observed. We were unable to find any change in Kondo effect after such adsorption−desorption cycles. Beside the local manipulations, we used a thermal method to switch back the Kondo effect by heating at 500 K, which induced the desorption of NO. After that, we took STM images and STS spectra in various locations of the sample and confirmed that the recovery of original CoTPP structures and Kondo effect had taken place.

To understand the on/off phenomena of the Kondo effect in the bimolecular reactions, we examined electronic and magnetic properties of CoTPP on Au(111), without and with the adsorbed NO molecule using the spin-polarized DFT calculation method as implemented in the Vienna Ab initio Simulation package (VASP).[40] Plane waves with the kinetic energy cutoff of 400 eV, projector-augmented wave (PAW) potentials,[41] and the Perdew−Burke−Ernzerhof (PBE)[42] exchange-correlation functional were used for our DFT simulations. For the Au(111) slab model, we used the p(6 × 6) surface unit cell (36 surface Au atoms) and three atomic layers. The work function of the Au(111) slab was calculated to be 5.29 eV, which is very close to experimental values of 5.1−5.5 eV.[43] The van der Waals interaction of CoTPP with Au(111) was corrected with the DFT-D2 method.[44]

Our DFT calculations show that an isolated CoTPP molecule is magnetic. The central $Co^{2+}$ ion with $d^7$ electrons exhibits a magnetic moment of 1 $\mu_B$, that is, occupying four majority spins and three minority spins, due to the crystal field made by the surrounding N terminals of the porphyrin backbone. When the CoTPP is placed on the Au(111) substrate, the orbital hybridization driven by the van der Waals interaction results in small electron transfer from Au to Co $d_{z^2}$ to form an electric dipole, thereby the total magnetic moment is reduced to 0.60 $\mu_B$. We believe that this net magnetic moment is the origin of the Kondo effect observed in our STS experiments. Molecular Kondo effect with magnetic moments smaller than 1.0 $\mu_B$ was previously reported.[27]

The adsorption and desorption of the NO molecule to and from Au(111)-supported CoTPP can happen *via* three configuration steps, as shown in Figure 5a: (1) nonbonding (NB), (2) vertical bonding (VB), and (3) tilted bonding (TB) geometries of NO. Electronic partial densities of states (PDOS) for the three configurations are plotted in Figure 5b. In the NB configuration, both the pp$\pi^*$ and $d_{z^2}$ orbitals of NO and CoTPP, respectively, are partially filled. The d orbital states

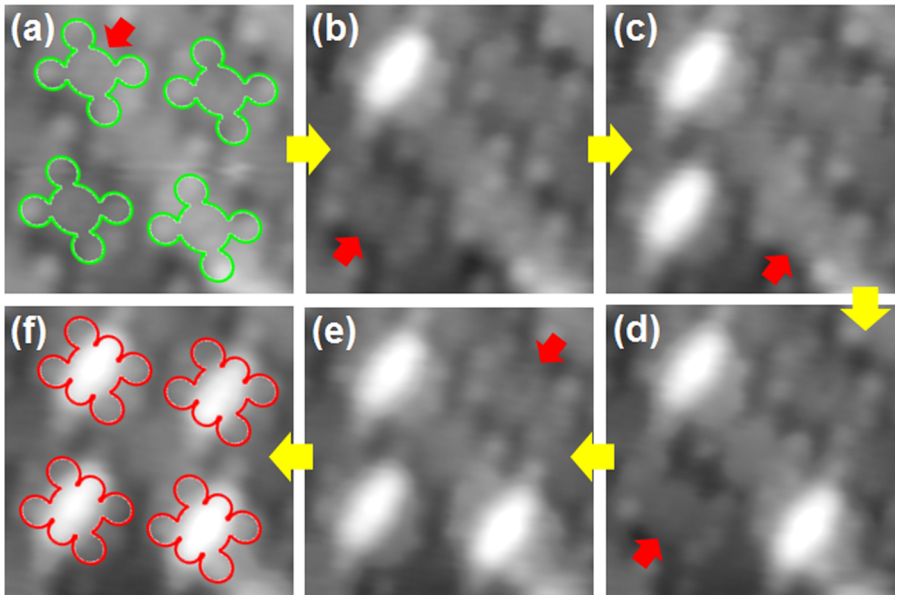


**Figure 4. Sequence of STM images from (a−f) demonstrating the reproducibility of the STM manipulation. Four NO−CoTPP and CoTPP are denoted by green and red, respectively, in (a) and (f). In each image, the target NO−CoTPP molecule is indicated by a red arrow. From (c) to (d), the detached NO was readsorbed onto the adjacent CoTPP. The tunneling conditions of all STM images are $I_T$ = 0.1 nA and $V_s$ = −0.5 eV.**

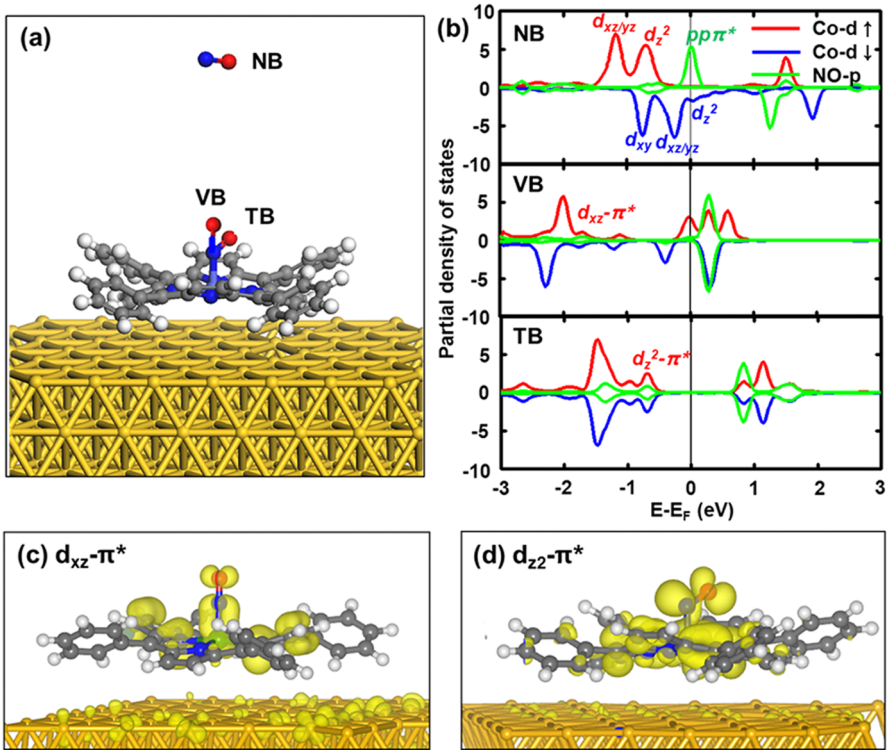


**Figure 5. (a) Overlapped atomic models of nonbonding (NB), vertical bonding (VB), and tilted bonding (TB) NO molecules on Au-supported CoTPP molecule. (b) Partial density of states (PDOS) for NB, VB, and TB configurations in (a). The Fermi level sets to the energy zero. Red, blue, and green lines indicate majority spin of Co d, minority spin of Co d, and NO p states, respectively. The charge density plot of the bonding states of (c) $d_{xz}$−$\pi$* and (d) $d_{z^2}$−$\pi$* in VB and TB configurations, respectively.**

between −1 eV and the Fermi level in Figure 5b did not appear in STS measurements, possibly due to limited sensitivity in tunneling matrix or due to limitations in DFT energy spacing in calculations. In the VB configuration, the high-lying pp$\pi$* orbital is exclusively hybridized with the low-lying $d_{xz}$ and $d_{yz}$ orbitals of Co, as evident from the charge density plot shown in Figure 5c. Yet, the $d_{z^2}$−$\pi$* coupling is forbidden in VB NO−CoTPP by symmetry. This VB configuration is metastable, mostly preserved by local four-fold symmetry. When the

**TABLE 1. Approximate Local Electron Configuration of the Co Ion and Calculated Total Magnetic Moments of CoTPP, NO−CoTPP, CO−CoTPP, and $O_2$−CoTPP Systems on Au(111)**

| | Co ion | magnetic moment ($\mu_B$) |
|---|---|---|
| CoTPP | $d^7$ | 0.60 |
| CO−CoTPP | $d^7$ | 0.94 |
| NO−CoTPP | $d^8$ | 0.00 |
| $O_2$−CoTPP | $d^6$ | 1.02 |

four-fold symmetry is largely broken, as in the saddle configuration or on Au(111) substrate, the VB configuration is spontaneously relaxed to TB configuration. TB configuration with one electron transfer from NO to CoTPP is the most stable structure with an energy gain of 1.53 eV, supported by the bonding character of the $d_{z^2}$−$\pi^*$ coupling, as shown in the charge density plot in Figure 5d. The up-shifted $\pi^*$ orbital loses its electron to the unoccupied, minority-spin $d_{z^2}$ orbital. Thus the NO-adsorbed CoTPP becomes nonmagnetic with fully paired $d^8$ electron configuration. The suppressed magnetic moment is induced by charge-transfer mechanisms upon NO adsorption, explaining the on/off Kondo behaviors observed in our STS experiments.

We further considered the possibility of spin control by the binding of $O_2$ or CO to CoTPP on Au(111) in our DFT calculations, as summarized in Table 1. Different from NO, we found that the magnetic moment of CoTPP could be switched off neither by $O_2$ nor by CO, and that the binding mechanisms of $O_2$ and CO were similar to those for TB and VB of NO to CoTPP, respectively. Paramagnetic triplet $O_2$ has two unpaired electrons in the pp$\pi^*$ orbital. When $O_2$ meets with CoTPP, the $\pi^*$ orbital attracts one electron from Co and hybridizes with the $d_{z^2}$ orbital of Co. While the Co ion becomes almost nonmagnetic with approximate $d^6$ configuration, the other unpaired electron still remains in the $\pi^*$ of $O_2$ to make the whole system magnetic with the net magnetic moment of 1.02 $\mu_B$. On the other hand, CO is nonmagnetic with the completely empty pp$\pi^*$ orbital. Still, the pp$\pi^*$ orbital of CO hybridizes with $d_{xz}$ and $d_{yz}$ orbitals of Co in the VB configuration without any charge transfer, preserving the local magnetic moment of Co. The electron configurations of Co thus become $d^7$ after binding of CO to CoTPP with the magnetic moment of 0.94 $\mu_B$. It will be interesting to see if the Kondo temperature is changed by $O_2$ or CO binding because they may change the spatial locations of net spin.

Recently, spin control over Mn−phthalocyanine (MnPc) was studied with the binding of CO on Bi(110) and atomic H on Au(111).[34,35] Noticeably, MnPc is a multiple spin system, whereas our CoTPP is a single spin system. In MnPc, Mn has two spins in $d_{z^2}$ and $d_{xy}$ orbitals on Bi(110) and three spins in $d_{xz}$/$d_{yz}$, $d_{z^2}$, and $d_{xy}$ orbitals on Au(111). The $d_{z^2}$ orbital hybridizes with the $\pi^*$ orbital of CO and s orbital of atomic H to reduce the net spin from 1 to 1/2 and from 3/2 to 1, respectively. Therefore, both CO−MnPc and H−MnPc are still magnetic with nonzero spins, very different from our NO−CoTPP case. It was argued that no Kondo effect after CO binding irrespective of remaining spin was the result of weak coupling of $d_{xy}$ orbital to substrate. In this regard, our NO−CoTPP system has the advantage that the mechanism of spin and Kondo switching is clear, intuitive, and suitable for model studies.

## CONCLUSION

In summary, we studied bimolecular chemical switching of the Kondo effect in CoTPP on Au(111) using NO molecules through STM and STS measurement. We observed reproducible transformations between three-lobed and bright ring structures from CoTPP molecules without and with adsorbed NO molecules in STM images, respectively. The bimolecular chemical switching could be made in both directions. The switching mechanism is attributed to the suppression of magnetic moment in NO−CoTPP on Au(111) from DFT analyses. The bimolecular chemical switching provides diverse options for controlling molecular Kondo effect because there are huge numbers of bimolecular sets for magnetic molecules and their counterparts.

## EXPERIMENTAL SECTION

All experiments were performed using our home-built STM system operating at 80 K with a base pressure of $1 \times 10^{-10}$ Torr. The Au(111) surface was prepared from a commercially available thin film (200 nm thick, PHASIS, Switzerland) of Au on mica that was exposed to several cycles of Ne-ion sputtering and annealing at 800 K. Commercially available CoTPP (Porphyrin Systems, Germany) and $H_2$TPP (Sigma Aldrich, USA) were outgassed in vacuum for several hours and then deposited on the Au(111) at submonolayer coverage by thermal evaporation using an alumina-coated evaporator. NO gas was introduced using a stainless steel tube (3 mm diameter) through a precision leak valve. STS spectra were obtained by a lock-in technique with a modulation voltage of 5 $mV_{rms}$ and at a frequency of 1.5 kHz.

*Conflict of Interest:* The authors declare no competing financial interest.

*Acknowledgment.* The authors gratefully acknowledge financial support from the National Research Foundation of Korea (Grant Nos. 2010-0025301 and 2010-0018781). Work at KAIST was supported by the NRF (2012R1A2A2A01046191) and Global Frontier R&D (2011-0031566) programs through the NRF of Korea. H.K. was supported by a Korea University Grant. Authors thank Mahn-Soo Choi and Ji-Yong Park for their helpful comments.

## REFERENCES AND NOTES

1. Joachim, C.; Gimzewski, J. K.; Aviram, A. Electronics Using Hybrid-Molecular and Mono-Molecular Devices. *Nature* **2000**, *408*, 541–548.

2. Bogani, L.; Wernsdorfer, W. Molecular Spintronics Using Single-Molecule Magnets. *Nat. Mater.* **2008**, *7*, 179–186.
3. Flechtner, K.; Kretschmann, A.; Steinrück, H.-P.; Gottfried, J. M. NO-Induced Reversible Switching of the Electronic Interaction between a Porphyrin-Coordinated Cobalt Ion and a Silver Surface. *J. Am. Chem. Soc.* **2007**, *129*, 12110–12111.
4. Gottfried, M.; Marbach, H. Surface-Confined Coordination Chemistry with Porphyrins and Phthalocyanines: Aspects of Formation, Electronic Structure, and Reactivity. *Z. Phys. Chem.* **2009**, *223*, 53–74.
5. Wäckerlin, C.; Chylarecka, D.; Kleibert, A.; Müller, K.; Iacovita, C.; Nolting, F.; Jung, T. A.; Ballav, N. Controlling Spins in Adsorbed Molecules by a Chemical Switch. *Nat. Commun.* **2010**, *1*, 61.
6. Hieringer, W.; Flechtner, K.; Kretschmann, A.; Seufert, K.; Auwärter, W.; Barth, J. V.; Görling, A.; Steinrück, H.-P.; Gottfried, J. M. The Surface Trans Effect: Influence of Axial Ligands on the Surface Chemical Bonds of Adsorbed Metalloporphyrins. *J. Am. Chem. Soc.* **2011**, *133*, 6206–6222.
7. Isvoranu, C.; Wang, B.; Ataman, E.; Knudsen, J.; Schulte, K.; Andersen, J. N.; Bocquet, M.-L.; Schnadt, J. Comparison of the Carbonyl and Nitrosyl Complexes Formed by Adsorption of CO and NO on Monolayers of Iron Phthalocyanine on Au(111). *J. Phys. Chem. C* **2011**, *115*, 24718–24727.
8. Isvoranu, C.; Wang, B.; Ataman, E.; Schulte, K.; Knudsen, J.; Andersen, J. N.; Bocquet, M.-L.; Schnadt, J. Ammonia Adsorption on Iron Phthalocyanine on Au(111): Influence on Adsorbate−Substrate Coupling and Molecular Spin. *J. Chem. Phys.* **2011**, *134*, 114710-10.
9. Miguel, J.; Hermanns, C. F.; Bernien, M.; Krüger, A.; Kuch, W. Reversible Manipulation of the Magnetic Coupling of Single Molecular Spins in Fe-Porphyrins to a Ferromagnetic Substrate. *J. Phys. Chem. Lett.* **2011**, *2*, 1455–1459.
10. Garthwaite, J. Glutamate, Nitric-Oxide and Cell−Cell Signaling in the Nervous System. *Trends Neurosci.* **1991**, *14*, 60–67.
11. Culotta, E.; Koshland, D. E. No News Is Good News. *Science* **1992**, *258*, 1862–1865.
12. Griffiths, C.; Garthwaite, G.; Garthwaite, J. The Glutamate Nitric Oxide Pathway in an *In Vitro* Model of Ischaemia. *Eur. J. Neurosci.* **1998**, *10*, 98–98.
13. Kadish, K. M.; Smith, K. M.; Guilard, R. *The Porphyrin Handbook*; Academic Press: New York, 1999.
14. Xue, L.; Farrugia, G.; Miller, S. M.; Ferris, C. D.; Snyder, S. H.; Szurszewski, J. H. Carbon Monoxide and Nitric Oxide as Coneurotransmitters in the Enteric Nervous System: Evidence from Genomic Deletion of Biosynthetic Enzymes. *Proc. Natl. Acad. Sci. U.S.A.* **2000**, *97*, 1851–1855.
15. Vizi, E. S.; Lajtha, A. *Handbook of Neurochemistry and Molecular Neurobiology: Neurotransmitter Systems*; Springer: Berlin, 2008.
16. Enemark, J. H.; Feltham, R. D. Principles of Structure, Bonding, and Reactivity for Metal Nitrosyl Complexes. *Coord. Chem. Rev.* **1974**, *13*, 339–406.
17. Scheidt, W. R.; Ellison, M. K. The Synthetic and Structural Chemistry of Heme Derivatives with Nitric Oxide Ligands. *Acc. Chem. Res.* **1999**, *32*, 350–359.
18. Wyllie, G. R. A.; Scheidt, W. R. Solid-State Structures of Metalloporphyrin $NO_x$ Compounds. *Chem. Rev.* **2002**, *102*, 1067–1089.
19. McCleverty, J. A. Chemistry of Nitric Oxide Relevant to Biology. *Chem. Rev.* **2004**, *104*, 403–418.
20. Ghosh, A. Metalloporphyrin−NO Bonding: Building Bridges with Organometallic Chemistry. *Acc. Chem. Res.* **2005**, *38*, 943–954.
21. Seufert, K.; Auwärter, W.; Barth, J. V. Discriminative Response of Surface-Confined Metalloporphyrin Molecules to Carbon and Nitrogen Monoxide. *J. Am. Chem. Soc.* **2010**, *132*, 18141–18146.
22. Burema, S. R.; Seufert, K.; Auwärter, W.; Barth, J. V.; Bocquet, M.-L. Probing Nitrosyl Ligation of Surface-Confined Metalloporphyrins by Inelastic Electron Tunneling Spectroscopy. *ACS Nano* **2013**, *7*, 5273–5281.
23. Kim, H.; Son, W. J.; Jang, W. J.; Yoon, J. K.; Han, S.; Kahng, S.-J. Mapping the Electronic Structures of a Metalloporphyrin Molecule on Au(111) by Scanning Tunneling Microscopy and Spectroscopy. *Phys. Rev. B* **2009**, *80*, 245402.
24. Iancu, V.; Deshpande, A.; Hla, S. W. Manipulating Kondo Temperature *via* Single Molecule Switching. *Nano Lett.* **2006**, *6*, 820–823.
25. Iancu, V.; Deshpande, A.; Hla, S. W. Manipulation of the Kondo Effect *via* Two-Dimensional Molecular Assembly. *Phys. Rev. Lett.* **2006**, *97*, 266603.
26. Li, Q.; Yamazaki, S.; Eguchi, T.; Kim, H.; Kahng, S. J.; Jia, J. F.; Xue, Q. K.; Hasegawa, Y. Direct Evidence of the Contribution of Surface States to the Kondo Resonance. *Phys. Rev. B* **2009**, *80*, 115431.
27. Perera, U. G. E.; Kulik, H. J.; Iancu, V.; da Silva, L. G. G. V. D.; Ulloa, S. E.; Marzari, N.; Hla, S. W. Spatially Extended Kondo State in Magnetic Molecules Induced by Interfacial Charge Transfer. *Phys. Rev. Lett.* **2010**, *105*, 106601.
28. Zhao, A. D.; Li, Q. X.; Chen, L.; Xiang, H. J.; Wang, W. H.; Pan, S.; Wang, B.; Xiao, X. D.; Yang, J. L.; Hou, J. G.; *et al.* Controlling the Kondo Effect of an Adsorbed Magnetic Ion through Its Chemical Bonding. *Science* **2005**, *309*, 1542–1544.
29. Gao, L.; Ji, W.; Hu, Y. B.; Cheng, Z. H.; Deng, Z. T.; Liu, Q.; Jiang, N.; Lin, X.; Guo, W.; Du, S. X.; *et al.* Site-Specific Kondo Effect at Ambient Temperatures in Iron-Based Molecules. *Phys. Rev. Lett.* **2007**, *99*, 106402.
30. Fu, Y. S.; Ji, S. H.; Chen, X.; Ma, X. C.; Wu, R.; Wang, C. C.; Duan, W. H.; Qiu, X. H.; Sun, B.; Zhang, P.; *et al.* Manipulating the Kondo Resonance through Quantum Size Effects. *Phys. Rev. Lett.* **2007**, *99*, 256601.
31. Choi, T.; Bedwani, S.; Rochefort, A.; Chen, C. Y.; Epstein, A. J.; Gupta, J. A. A Single Molecule Kondo Switch: Multistability of Tetracyanoethylene on Cu(111). *Nano Lett.* **2010**, *10*, 4175–4180.
32. Tsukahara, N.; Shiraki, S.; Itou, S.; Ohta, N.; Takagi, N.; Kawai, M. Evolution of Kondo Resonance from a Single Impurity Molecule to the Two-Dimensional Lattice. *Phys. Rev. Lett.* **2011**, *106*, 187201.
33. Komeda, T.; Isshiki, H.; Liu, J.; Zhang, Y. F.; Lorente, N.; Katoh, K.; Breedlove, B. K.; Yamashita, M. Observation and Electric Current Control of a Local Spin in a Single-Molecule Magnet. *Nat. Commun.* **2011**, *2*, 217.
34. Stróżecka, A.; Soriano, M.; Pascual, J. I.; Palacios, J. J. Reversible Change of the Spin State in a Manganese Phthalocyanine by Coordination of Co Molecule. *Phys. Rev. Lett.* **2012**, *109*, 147202.
35. Liu, L.; Yang, K.; Jiang, Y.; Song, B.; Xiao, W.; Li, L.; Zhou, H.; Wang, Y.; Du, S.; Ouyang, M.; *et al.* Reversible Single Spin Control of Individual Magnetic Molecule by Hydrogen Atom Adsorption. *Sci. Rep.* **2013**, *3*, 1210.
36. Auwärter, W.; Seufert, K.; Klappenberger, F.; Reichert, J.; Weber-Bargioni, A.; Verdini, A.; Cvetko, D.; Dell'Angela, M.; Floreano, L.; Cossaro, A.; *et al.* Site-Specific Electronic and Geometric Interface Structure of Co-Tetraphenyl-Porphyrin Layers on Ag(111). *Phys. Rev. B* **2010**, *81*, 245403.
37. Fano, U. Effects of Configuration Interaction on Intensities and Phase Shifts. *Phys. Rev.* **1961**, *124*, 1866.
38. Nagaoka, K.; Jamneala, T.; Grobis, M.; Crommie, M. F. Temperature Dependence of a Single Kondo Impurity. *Phys. Rev. Lett.* **2002**, *88*, 077205.
39. Groombridge, C. J.; Larkworthy, L. F.; Mason, J. Swinging of the Bent Nitrosyl Ligand in [Co($^{15}$NO)(TPP)]: A Solid-State Motion Detected by $^{15}$N CPMAS NMR Spectroscopy. *Inorg. Chem.* **1993**, *32*, 379–380.
40. Kresse, G.; Furthmüller, J. Efficiency of Ab-Initio Total Energy Calculations for Metals and Semiconductors Using a Plane-Wave Basis Set. *Comput. Mater. Sci.* **1996**, *6*, 15–50.
41. Blöchl, P. E. Projector Augmented-Wave Method. *Phys. Rev. B* **1994**, *50*, 17953–17979.
42. Perdew, J. P.; Burke, K.; Ernzerhof, M. Generalized Gradient Approximation Made Simple. *Phys. Rev. Lett.* **1996**, *77*, 3865–3868.
43. Tseng, C. T.; Cheng, Y. H.; Lee, M. C. M. Study of Anode Work Function Modified by Self-Assembled Monolayers on Pentacene/Fullerene Organic Solar Cells. *Appl. Phys. Lett.* **2007**, *91*, 233510.
44. Grimme, S. Semiempirical GGA-Type Density Functional Constructed with a Long-Range Dispersion Correction. *J. Comput. Chem.* **2006**, *27*, 1787–1799.